Microstructural effects on surface mechanical properties of ion-implanted polymers

G. R. Rao, Z. L. Wang, and E. H. Lee
Metals and Ceramics Division, P.O. Box 2008, Oak Ridge National Laboratory, Oak Ridge, Tennessee 37831-6376

(Received 16 December 1991; accepted 7 December 1992)

Tefzel, a copolymer of tetrafluoroethylene and ethylene, was implanted simultaneously with 400 keV boron, 700 keV nitrogen, and 600 keV carbon to a dose of 3×10^{15} ions/cm^2 for each ion. The implanted layer was examined using transmission electron microscope and compared with the pristine Tefzel for microstructural changes. The microhardness of the implanted and pristine Tefzel was determined using a nanoindentation technique. TEM bright-field images of the implanted layer show a patch-type contrast with distinguishable bright and dark regions. Electron energy loss spectroscopy (EELS) was used to show that the bright regions had a higher carbon concentration, as compared with the dark regions. The carbon-rich regions had an average size of approximately 40 nm. The pristine material showed a fairly featureless contrast with occasional local patchy regions. These were determined to be due to local thickness variations. The triple implantation improved the hardness of pristine Tefzel by over 66 times. The structure of the carbon-rich regions appears to be clusters of sp^2 bonded C atoms with sp^3 sites present and hydrogen preferentially bonded in the sp^3 C configuration. It was speculated that the carbon-rich regions could be harder than the surrounding regions, but this could not be resolved due to the small size of the regions.

I. INTRODUCTION

Recent studies at Oak Ridge National Laboratory have shown that ion-beam treatment of polymers can dramatically improve surface properties such as hardness and wear resistance. In particular, it has been shown that multiple ion implantation is more effective than single ion implantation.[1] Currently, there is significant interest in understanding these changes caused by ion irradiation at the microstructural level, to comprehend better the macroscopic effects in polymers.

Ion implantation induces various changes in the structure and chemistry of polymers. Residual gas analysis has shown that there is a liberation of various gaseous species such as hydrogen, carbon monoxide, carbon dioxide, and an assortment of hydrocarbons during irradiation, particularly in the initial stages.[1] This leads to a reorganization of the near-surface structure and chemistry. It has been shown that the irradiation results in the formation of a carbonized layer on the surface.[2,3] The structure of this carbon-rich layer is of interest in understanding the effects of the irradiation since it is directly responsible for the surface property changes. Our current knowledge regarding surface microstructure of ion-implanted polymers comes mainly from work done on conductivity enhancement in polymers by ion implantation. The current model for conductivity enhancement is based on the presence of carbon-rich islands separated by insulating channels. Conductivity occurs by an "electronic hopping mechanism" wherein electrons "tunnel" through the insulating channels while moving from island to island.[4] Only indirect evidence was found for the presence of these islands. Recently, Fink *et al.* were able to show, using neutron scattering experiments, the presence of small globular carbon clusters with an average radius of 6 to 7 nm, separated by an average distance of 13 nm in the matrix.[5]

The aim of the present study is to explore the possibility of the presence of such carbon-rich regions in multiple-ion-implanted polymers, to obtain visual evidence of these regions using transmission electron microscopy (TEM), and to study the structure by electron energy loss spectroscopy (EELS). A further goal is to relate the structure and composition of the carbon-rich regions to the macroscopic surface property changes.

II. EXPERIMENTAL

Tefzel, a copolymer of tetrafluoroethylene and ethylene, in the form of a film of average thickness of 127 μm was selected for this study. The structure of this polymer is shown in Fig. 1. The polymer was obtained from the DuPont company. The polymer film was irradiated simultaneously with 400 keV boron, 700 keV nitrogen, and 600 keV carbon ions to a dose of 3×10^{15} ions/cm^2 for each ion. Specimen temperature was consistently maintained under 100 °C by limiting the beam current to less than 100 nA/cm^2. The irradiations

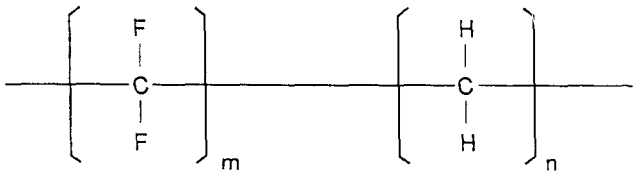

TEFZEL

FIG. 1. Molecular structure of Tefzel, a copolymer of tetrafluoroethylene and ethylene used for the implantations.

were carried out using the Van de Graaff accelerators in the triple-ion irradiation facility in the Metals and Ceramics Division at Oak Ridge National Laboratory.[6]

Hardness measurements were performed using the Nanoindenter™ microindentation system. The Nanoindenter is a completely automated system that determines hardness from dynamic load and displacement measurements. This eliminates uncertainties associated with optical measurements of indents needed for conventional microhardness tests such as Knoop and Vickers. The system has 300 nN force and 0.4 nm displacement resolutions and continually monitors the load and displacement during the indentation. The actual indentation depth was set at 500 nm with a displacement rate of 10 nm/s. Unloading was performed at a rate of 7 nm/s until the load reached 10% of the maximum value. The indenter was held at this position for 25 s to determine the drift rate and then the unloading was completed.

Transmission electron microscope specimens were obtained by embedding the implanted polymer film in epoxy and taking cross-sectional slices of thickness 70–100 nm using an RMC ultramicrotome. The specimens were examined in a Phillips CM12 (120 kV) TEM. Electron energy loss spectra were obtained using a parallel EELS detector system (Gatan model 666) on a Phillips EM400T TEM/STEM (100 kV) equipped with a field emission gun. The EELS spectra were acquired in the diffraction mode with a small electron probe of about 3 nm diameter. It took about 20 s to acquire a core-shell ionization spectrum and 2 s to acquire a low-loss spectrum.

III. RESULTS

A. Changes during irradiation

The surface color of Tefzel changed continually from colorless for the pristine material to blackish at the conclusion of the irradiation. This effect is observed in all the polymers we have irradiated and is ascribed to the release of gases and the formation of a carbon-rich layer during the implantation. The surface of the implanted polymer was smoother than for the pristine material when observed under an optical microscope.

During the irradiation of polymers, an increase in chamber pressure is usually observed in the first few minutes of the irradiation. The ultrahigh vacuum chamber was initially maintained at around 1.5×10^{-8} Torr. At the beginning of the irradiation, pressure was found to increase by one or two orders of magnitude due to the emission of gases from the polymer surface.[8] Residual gas analysis (RGA) has been used earlier to identify gases emitted during the irradiation of polymers.[1,8] While RGA was not performed during the B, N, C implantation of Tefzel, it was used in an earlier study during a 200 keV Si^+ implantation of Tefzel. The results of the analysis are shown in Table I. It has been shown that even though the absolute yield of the gaseous molecular emissions depends upon ion current, energy and mass, relative yields depend mainly upon polymer type.[1] Therefore, the data shown in Table I would probably not be too different for the B, N, C implanted case.

B. TEM and EELS

Figure 2 shows typical TEM bright-field images obtained for the pristine and B, N, C implanted Tefzel. A patch-type contrast is observed showing dark and bright regions in the implanted sample, whereas the pristine material shows a uniform, basically featureless contrast, although some localized patch-type contrast is also observed. The observed contrast could be interpreted in two ways. It could be due to a mass-thickness variation across the specimen. Alternatively, it could be the result of a variation in the local atomic concentrations with a fairly uniform specimen thickness. The EELS was used to decide which of the two interpretations was correct.

Various inelastic scattering processes can be excited by a fast electron beam passing through the specimen such as plasmon and core-shell ionization edges. These different processes can be used to characterize the atomic structure of the specimen. The dielectric properties are usually contained in plasmon-loss spectra, generated by collective excitations of electrons in the solid, resulting

TABLE I. Residual gas analysis (RGA) results showing molecular emission products during 200 keV Si ion implantation.[a]

Mass number	Molecular species	Relative chemical yield[b]
2	H_2	10
20	HF	9
26	C_2H_2	2
31	CF	2.3
50	CF_2	1.6
69	CF_3	0.8

[a]From Ref. 1.
[b]Relative chemical yield was measured by the increment of ion current above background.

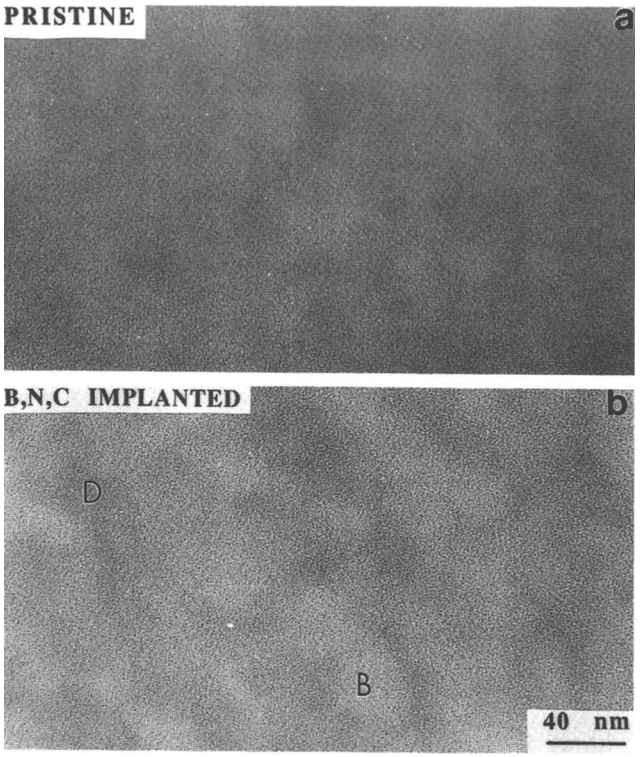

FIG. 2. Typical transmission electron micrographs obtained for pristine (a) and B, N, C implanted (b) Tefzel. The implanted specimen shows bright (B) and dark (D) patches, which correspond to the microstructures of implanted Tefzel (see text).

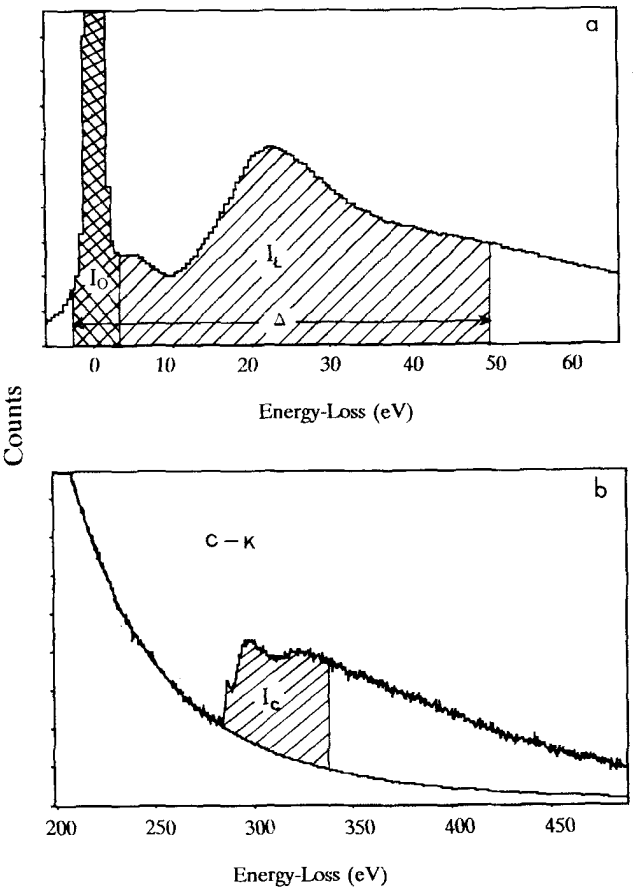

FIG. 3. Parts (a) and (b) are EELS spectra acquired from the same specimen area for low energy-loss and C-K edge loss, respectively. The shadowed areas are used for quantitative analysis (see text for details). The background intensity is drawn in (b).

in low energy-losses, typically about 10–30 eV. Core-shell ionization edges are generated by transitions of electrons from atomic inner shells to the unoccupied states, the corresponding intensity being proportional to the concentration of the atoms in the specimen so that it can be used for quantitative chemical composition analysis. Furthermore, the shape of the core-shell ionization edge is closely related to the density of states in the conducting band, and contains the electronic structure information of the solid.

In EELS, the integrated intensity of the core-ionization edge, $I_c(\Delta)$, for an energy window Δ (Fig. 3) is related to the integrated intensity of the low energy-loss part, $I_L(\Delta)$, by Eq. (1)[9]:

$$I_c(\Delta) = I_L(\Delta) \cdot \sigma_c(\Delta\beta)nt, \qquad (1)$$

where σ_c is the ionization cross section of the core edge for a collection semi-angle β, n is the corresponding atom concentration for the measured core loss, and t is the specimen thickness. If the angle β is much larger than the inelastic scattering characteristic angle $\Theta_E \approx \Delta E/2E_0$ of the valence loss, typically about 0.1 mrad for $\Delta E = 20$ eV and $E_0 = 100$ kV, so that the multiple inelastic scattering is described by the Poisson distribution, the specimen thickness can be determined by Eq. (2)[10]:

$$t = \lambda \ln\left(\frac{I}{I_0}\right), \qquad (2)$$

where I_0 and I are the integrated intensity of the zero-loss peak and the entire spectrum, respectively, and λ is the electron inelastic scattering mean free path (Fig. 4). From Eqs. (1) and (2), the local atomic concentration is determined by:

$$n = \frac{k}{\sigma_c \lambda}, \quad \text{where } k = \frac{I_c}{I_L \ln\left(\frac{I}{I_0}\right)}. \qquad (3)$$

For thin specimens, σ_c and λ usually do not depend on specimen thickness. Therefore, the variation of the k factor across the specimen directly reflects the change in local chemical composition. Based on Eq. (3), the variation of the carbon concentration from the dark and bright regions in the TEM bright-field images was determined.

Table II shows the experimentally measured k factors for the bright (B) and the dark (D) contrast

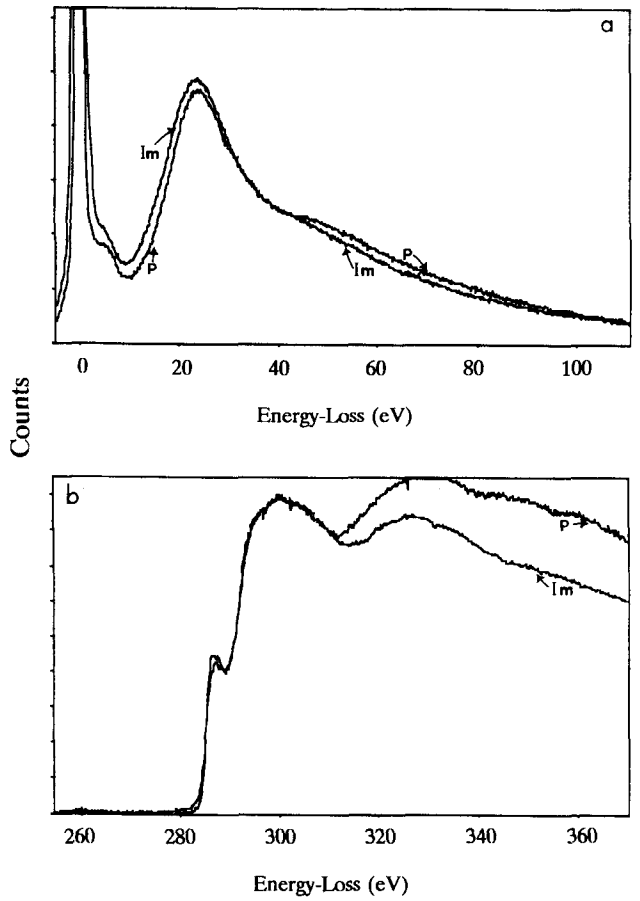

FIG. 4. Comparison of EELS spectra acquired for pristine Tefzel (P) and implanted Tefzel (Im) for (a) low energy-loss part and (b) C-K edge after the subtraction of background. The spectra in (b) are normalized at the intensity for energy-loss $\Delta E = 300$ eV for comparison purposes since the number of counts does not represent absolute intensity.

patches across the pristine and implanted specimens for different thicknesses. In the implanted specimen, for thin regions, the variation of t/λ is less than 2% for adjacent bright and dark regions, whereas the variation of the k factor is more than 15%. This indicates that the average carbon concentration in the bright region is about 15% greater than in the dark regions. For relatively thicker regions, the thickness variation of the bright and dark regions varied by up to 10%. However, the carbon concentration is always higher in the bright contrast area as compared with the dark regions. On the other hand, for the pristine polymer, it can be seen from Table II that the variation of k was always under 5%. The small patches observed in some regions must be due to local thickness variations.

In EELS, the intensity variation within about 10 eV close to the core edge threshold is the so-called energy loss near edge structure (ELNES), which is mostly related to the density of the states. This part is usually not sensitive to multiple scattering effects. For energy losses far from the edge threshold, the intensity variation is partly determined by the change of atom environment, such as nearest neighbor distribution and partly by the multiple scattering effect. To rule out the latter part, we have carefully selected the specimen areas in the implanted and nonimplanted Tefzel regions so that the multiple scattering effect would have similar results in the spectra. Figure 4(a) shows the comparison of the low energy-loss part from the pristine and the bright regions in the implanted Tefzel.

TABLE II. Experimentally measured t/λ and k factors from EELS spectra for the bright and dark regions in the TEM micrographs at different regions.

Measurement	Contrast[a]	t/λ	k ($\times 10^{-3}$)	$(n_B - n_D)/n_D = (k_B - k_D)/k_D$[b]
Pristine Tefzel				
1	D	1.0	0.5	
	B	1.22	0.512	2.4%
2	D	1.36	0.579	
	B	1.34	0.596	2.9%
3	D	1.25	0.604	
	B	1.32	0.583	3.6%
4	D	1.01	0.5705	
	B	1.08	0.576	1.0%
B, N, C implanted Tefzel				
1	D	0.63	6.14	
	B	0.61	7.29	18.7%
2	D	0.89	5.17	
	B	0.90	5.97	15.4%
3	D	1.24	4.90	
	B	1.12	5.24	6.9%
4	D	1.73	4.57	
	B	1.46	5.27	15.3%

[a]D represents the dark regions and B the bright regions in the TEM micrographs. For each measurement, spectra were obtained from adjacent dark and bright regions.
[b]Represents percentage difference in carbon concentration for each measurement.

C. Hardness

The average hardness values at 100 nm depth for the pristine and B, N, C implanted Tefzel are shown in Fig. 5. The hardness of Fe^+ implanted Tefzel is also shown for comparison.[1] The B, N, C implanted Tefzel shows an increase in hardness of nearly 70 times (over 4600%), as compared to the pristine material. Hardness is computed as the applied load divided by the actual contact area. Actual contact area is determined by obtaining the actual contact depth from the x-axis intercept of the tangent to the unloading curve in the load-displacement plot. This technique for hardness estimation is described in Refs. 11 and 12. The exact

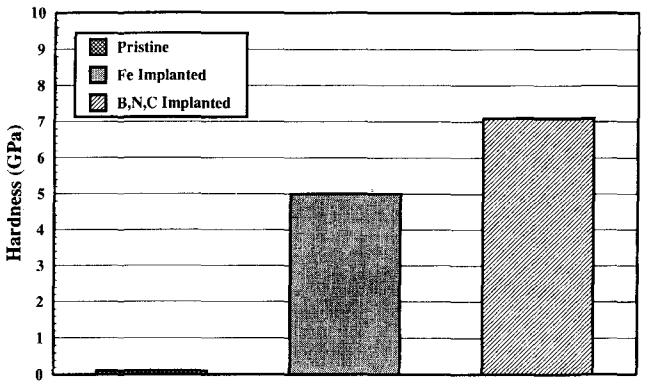

FIG. 5. Average hardness values for pristine and B, N, C implanted Tefzel compared to the hardness of Fe implanted Tefzel (from Ref. 1).

geometry of the diamond indenter tip was experimentally determined so that the actual contact area could be computed. The hardness value at 100 nm depth was taken as a standard for comparison. The indentation depth of 100 nm minimizes the magnitude of errors associated with shallower depths and avoids substrate effects at greater depths.[13]

IV. DISCUSSION

Ion bombardment at high energies drastically affects the chemistry and microstructure of the surface of polymers. This is eventually responsible for the large changes obtained for mechanical, physical, and chemical properties. The major effects of ion bombardment are (1) excitation and ionization of host atoms, (2) formation of radicals which enhance chemical activity, (3) loss of gaseous molecules which causes enrichment of specific elements on the polymer surface, (4) chain scission, which includes side chain scission and main backbone chain scission, (5) cross-linking, and (6) formation of precipitate particles due to the interaction of the implanted ions with other species in the polymer. These processes occur simultaneously and essentially lead to a microstructural reorganization at the polymer surface. They also depend upon ion energy used. At higher energies, there are mainly electronic energy absorption mechanisms dominant that lead to ionization. Ion-atom collisions at lower energies are responsible for most of the structural rearrangement.

A. Microstructure

The TEM micrographs and EELS analyses clearly show that there are two regions of different concentrations of C atoms on the B, N, C implanted Tefzel surface. For amorphous materials, the contrast introduced by electron diffraction effects can be completely neglected. Phase contrast can introduce fine details at the atomic level but should not produce any patch-type contrast in the large scale. This fact has been confirmed experimentally by examining an amorphous carbon film in the TEM and noting that no contrast variation was observed. In the case of implanted Tefzel, contrast change was observed by tilting the specimen by about 5°, which caused expansion or contraction of the patch size. This indicates localized ordered structure. It is obvious that the spectra almost follow the same shape. However, the core-shell edge of C-K from the same areas shows quite different shapes at the extended energy-loss part from 300–340 eV [Fig. 3(b)]. The difference cannot be attributed to multiple scattering effect. The only possible interpretation is a difference in the structure of the solid. Fine structures in EELS spectra of diamond, amorphous carbon, and graphite have been examined.[14] None of them showed a strong broadened peak located at 300 keV, as observed in Fig. 4. However, it is surprising to find that the 300 eV peak does appear in the EELS spectra of the solid form of C_{60}-fullerene.[15]

Figure 6 shows the atomic enrichment factors (defined as the ratio of atomic fraction in the virgin polymer to atomic fraction in the emission products) for carbon, fluorine, and hydrogen in 200 keV Si^+ ion-implanted Tefzel. The C-enrichment factor was found to be over two.[1] Our study clearly shows that the bright regions observed in the TEM images of B, N, C implanted Tefzel have a carbon concentration of up to 15% higher, as compared with the darker regions. This segregation of carbon-rich regions is consistent with currently understood mechanisms for the enhancement of conductivity of polymers using ion beams. The model due to Sheng and Abeles involves charge transport by hopping between carbon-rich conducting islands separated by the insulating matrix.[16] Foti and Reitano have reported the formation of ordered clusters of carbon in 240 keV Ar^+ implanted polystyrene, which grew with increasing dose.[17] Recently, Fink *et al.* have used neutron scattering experiments to prove the existence of carbon

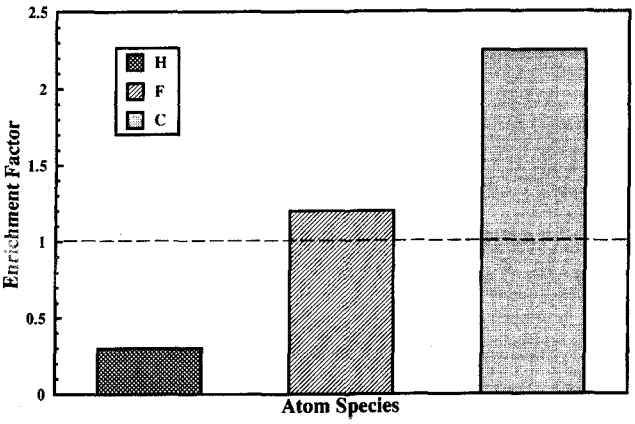

FIG. 6. The atomic enrichment factor for carbon, fluorine, and hydrogen after 200 keV Si implantation in Tefzel (after Ref. 1).

particles on the surface of 50 MeV boron-implanted Mylar foils.[5] They determined the radius of the globular carbon particles to be 6 to 7 nm, and they suggest that these particles coagulate to form larger clusters. The particles were found to be separated by an average distance of 13 nm in the matrix. A rough estimate from TEM micrographs in this study showed that the average size of the bright carbon-rich regions was around 40 nm, which is consistent within the framework of the conduction model for ion-implanted polymers.[5,16]

Studies have shown that ion-beam implantation produces a surface structure very similar to hydrogenated amorphous carbon.[2,3,18] This is also the case for B, N, C implanted Tefzel, as determined by comparing EELS spectra of the implanted sample with that of amorphous carbon.[14] The structure has been visualized to be a network of independent clusters of sp^2 bonded carbon atoms, with sp^3 sites being present and hydrogen preferentially bonded in the sp^3 carbon configuration.[19]

Raman spectra were obtained for the pristine and B, N, C implanted Tefzel earlier and are shown in Fig. 7.[1] The spectrum for the implanted Tefzel shows two peaks at 1356 and 1588 cm^{-1}. These are termed the D and G peaks, respectively. The D peak is associated with polycrystalline graphite which has medium-range order. The intensity of the D peak is proportional to the inverse of the effective crystallite size[19]:

$$I_D \propto \frac{1}{L_a} \tag{4}$$

The G peak comes from small crystals and has been shifted up from 1580 cm^{-1}, the wave number for a large single crystal, due to the small crystal size.[19] Tuinstra and Koenig have established a linear relationship between the ratio of the intensities $I(D)/I(G)$ and $1/L_a$, where the crystallite size L_a was obtained by x-ray diffraction.[20] Using this relationship, the crystallite size L_a has been determined to be around 6 nm for the B, N, C implanted Tefzel in our study. It is likely that the carbon-rich regions (bright regions observed in the TEM) are made of small crystallites, as also suggested by Foti and Reitano[17] and Fink *et al.*[5]

B. Hardness

The improvement in hardness of the implanted polymer has been suggested to be due to three major mechanisms: (1) three-dimensional cross-linking due to scission of side groups and chains, (2) introduction of alloying elements to form new chemical links which further enhance the cross-linking, and (3) embedding hard particles.[1] It has been shown in this paper that the surface of the polymer was carbonized by the formation of carbon-rich clusters. The carbon-rich regions have a mixture of sp^2 and sp^3 type bonding. The sp^3 tetrahedral

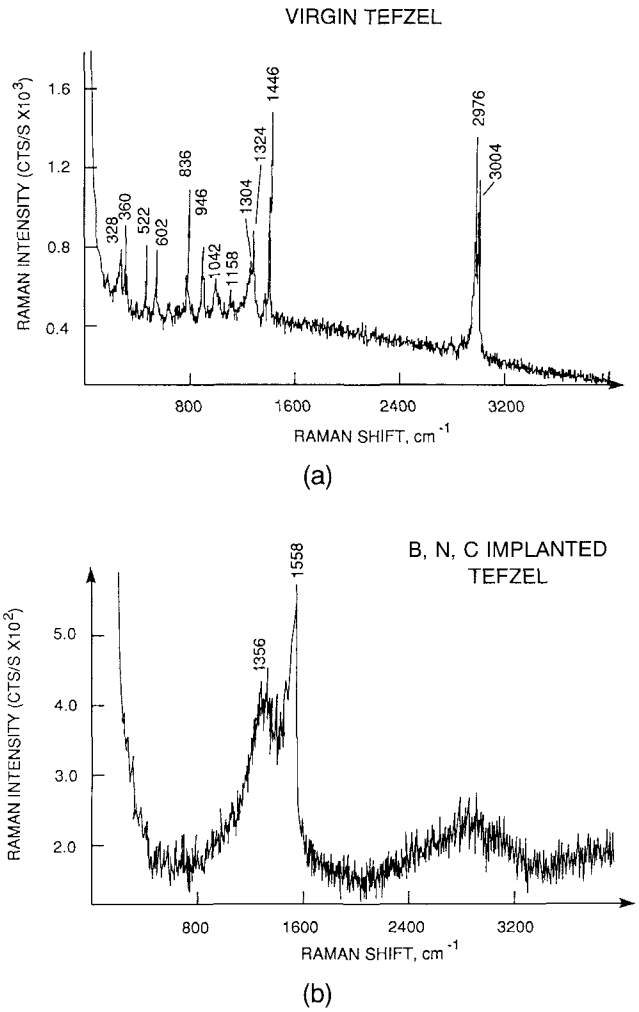

FIG. 7. Raman spectra obtained for pristine (a) and implanted (b) Tefzel. The implanted Tefzel spectrum shows the characteristic twin peaks at 1356 cm^{-1} (D peak) and 1588 cm^{-1} (G peak) similar to the spectra for amorphous carbon with short-range order.

bonding would be expected to contribute significantly to the hardness of the implanted layer.

It has been shown that there exists a remarkable correlation between carbon enrichment and hardness improvement in ion-implanted polymers.[1] This indicates that the carbon-rich regions play a major role in hardness improvement. The sp^3/sp^2 ratio is thus an important factor contributing to the hardness and the ratio has been found to be significant in as-grown amorphous hydrogenated carbon.[21] In the surrounding matrix region, covalent cross-linking probably plays the major role. While the ratio of sp^3/sp^2 bonds could not be estimated in this study, it is conceivable, depending upon the percentage fraction of sp^3 bonds, that the carbon-rich regions may actually be harder than the surrounding cross-linked matrix regions. This is difficult to measure experimentally because of the dimensions of the carbon-rich regions. The average size of these regions, as

observed by TEM, is around 40 nm. However, the projected area of contact of the nanoindenter at a 100 nm depth of indentation, at which hardness is calculated, is about 550 nm^2. The hardness value estimated is therefore an overall average of the carbon-rich clusters and the matrix material.

V. CONCLUSIONS

In this study, Tefzel (tetrafluoroethylene-ethylene copolymer) was implanted simultaneously with boron, nitrogen, and carbon. The implanted layer was examined in a transmission electron microscope and electron energy loss spectroscopy was used to determine the structure. A nanoindentation technique was used to determine surface hardness changes. The following conclusions resulted from this study:

(1) TEM bright-field images of the B, N, C implanted Tefzel showed a patch-type contrast with bright and dark regions. Pristine Tefzel revealed a fairly featureless contrast, but with localized patchy regions.

(2) EELS showed that the bright regions in the TEM images of the implanted layer had a higher carbon concentration, as compared with the dark regions indicating the clustering of carbon. The carbon-rich regions had an average size of approximately 40 μm. The patches observed in the pristine material were determined to be due to local thickness variations.

(3) EELS indicated that the implanted surface was similar to amorphous carbon, as observed by other researchers.

(4) The surface of Tefzel showed a factor of 70 increase in hardness after implantation. The carbon-rich regions are probably harder than the surrounding regions due to the presence of sp^3 (diamond-type) tetrahedral bonds. However, this could not be resolved due to the small size of the carbon-rich regions.

ACKNOWLEDGMENTS

The authors would like to thank Mr. S. W. Cook for the implantations and Dr. E. A. Kenik and Dr. M. B. Lewis of ORNL for technical review of the manuscript. This research was sponsored in part by the United States Department of Energy, Assistant Secretary for Conservation and Renewable Energy, Office of Industrial Technologies, Advanced Industrial Concepts (AIC) Materials Program, and in part by the Division of Materials Sciences, United States Department of Energy, under Contract No. DE-AC-05–84OR21400 with Martin Marietta Energy Systems Inc.

REFERENCES

1. E. H. Lee, M. B. Lewis, P. J. Blau, and L. K. Mansur, J. Mater. Res. **6**, 610–628 (1991).
2. J. Davenas, P. Thevenard, G. Boiteux, M. Fallavier, and X. L. Lu, Nucl. Instrum. Methods **B46**, 322 (1990).
3. G. Compagnini, R. Reitano, L. Calcagno, G. Marletta, and G. Foti, Appl. Surf. Sci. **43**, 231 (1989).
4. A. J. Lovinger, S. R. Forrest, M. L. Kaplan, P. H. Schmidt, and T. Venkatesan, J. Appl. Phys. **55** (2), 480–481 (1984).
5. D. Fink, K. Ibel, P. Goppelt, J. P. Biersack, L. Wang, and M. Behar, Nucl. Instrum. Methods **B46**, 345 (1990).
6. M. B. Lewis, W. R. Allen, R. A. Buhl, N. H. Packan, S. W. Cook, and L. K. Mansur, Nucl. Instrum. Methods **B43**, 243 (1989).
7. W. C. Oliver, Mater. Res. Bull. September/October, 15 (1986).
8. M. B. Lewis and E. H. Lee, Nucl. Instrum. Methods **B61**, 457 (1991).
9. R. F. Egerton, *Electron Energy-Loss Spectroscopy in the Electron Microscope* (Plenum Press, New York, 1986).
10. M. Creuzburg and H. Dimigen, Z. Phys. **174**, 24 (1963).
11. J. B. Pethica, R. Hutchings, and W. C. Oliver, Philos. Mag. A **48** (4), 593 (1983).
12. M. F. Doerner and W. D. Nix, J. Mater. Res. **1**, 601 (1986).
13. E. H. Lee, Y. Lee, W. C. Oliver, and L. K. Mansur, J. Mater. Res. **8**, 377–387 (1993).
14. R. F. Egerton and M. J. Whelan, J. Electron Spectrosc. **3**, 232–236 (1974).
15. P. L. Hansen, P. J. Fallon, and W. Krätschmer, Chem. Phys. Lett. **181** (4), 368 (1991).
16. T. Venkatesan, R. C. Dynes, B. Wilkens, A. E. White, J. M. Gibson, and R. Hamm, in *Ion Implantation and Ion Beam Processing of Materials*, edited by G. K. Hubler, O. W. Holland, C. R. Clayton, and C. W. White (Mater. Res. Soc. Symp. Proc. **27**, Elsevier Science Publishing, New York, 1984), p. 449.
17. G. Foti and R. Reitano, Nucl. Instrum. Methods **B46**, 307 (1990).
18. L. Calcagno and G. Foti, Nucl. Instrum. Methods **B59/60**, 1153–1158 (1991).
19. J. Robertson and E. P. O'Reilly, Phys. Rev. B **35** (6), 2953 (1987).
20. P. Tuinstra and J. L. Koenig, J. Chem. Phys. **53** (3), 1128 (1970).
21. B. Dischler, A. Bubenzer, and P. Koidl, Solid State Commun. **48** (2), 107 (1983).